The Astronomical Journal, 121:3041–3047, 2001 June

MULTIPLE COMPONENTS OF THE LUMINOUS COMPACT X-RAY SOURCE AT THE EDGE OF HOLMBERG II OBSERVED BY *ASCA* AND *ROSAT*

Takamitsu Miyaji
Department of Physics, Carnegie Mellon University, 5000 Forbes Avenue, Pittsburgh, PA 15213-3890; miyaji@astro.phys.cmu.edu
Ingo Lehmann[1]
Department of Astronomy and Astrophysics, Pennsylvania State University, University Park, PA 16802; ilehmann@aip.de
and
Günther Hasinger
Astrophysikalisches Institut Potsdam, An der Sternwarte 16 D-14482, Potsdam, Germany; ghasinger@aip.de
Received 2001 January 3; accepted 2001 February 28

ABSTRACT

We report the results of the analysis of new *ASCA* observations and archival *ROSAT* data of the compact luminous X-ray source found at the edge of the nearby star-forming dwarf galaxy Holmberg II (UGC 4305) in the M81 group. We have found a number of new features in the X-ray properties of this source. Our new *ASCA* spectrum revealed that the X-ray emission extends to the hard band and can be best described by a power law with a photon spectral index $\Gamma \sim 1.9$, while a $kT \sim 5$ keV thermal plasma with a low abundance ($\sim 0.2\ Z_\odot$) is also acceptable. The *ASCA* spectrum does not fit with a multicolor disk blackbody, unlike some off-nucleus X-ray sources with similar luminosities. The joint *ASCA*-*ROSAT* spectrum suggests two components to the spectrum: the hard power-law component and a warm thermal plasma ($kT \sim 0.3$ keV). An additional absorption over that of our galaxy is required. The wobble correction of the *ROSAT* HRI image has clearly unveiled the existence of an extended component that amounts to 27% $\pm$ 5% of the total X-ray emission. These observations indicate that there are more than one component in the X-ray emission. The properties of the pointlike component indicate an accretion onto an intermediate-mass black hole unless a beaming is taking place. We argue that the extended component does not come from electron scattering and/or reflection by scattered optically thick clouds of the central radiation. Possible explanations of this X-ray source include multiple supernova remnants feeding an intermediate-mass black hole.

Key words: galaxies: individual (Holmberg II) — X-rays

1. INTRODUCTION

Off-nuclear (not active galactic nuclei [AGN]) pointlike luminous X-ray sources, which exceed the Eddington luminosity of a usual stellar-mass compact object such as neutron stars and Galactic binary black holes ($L_x \gtrsim 10^{39}$ ergs s^{-1}) in nearby galaxies have been recognized in many galaxies (Fabbiano 1989; Colbert & Mushotzky 1999; Read, Ponman, & Strickland 1997). The luminosity distribution of these sources extends up to a few times 10^{40} ergs s^{-1}. The most luminous one has been found in the nuclear region of the starburst galaxy M82 (Ptak & Griffiths 1999; Matsumoto & Tsuru 1999), reaching $\sim 10^{41}$ ergs s^{-1}. The location of this source was recently verified by *Chandra* to be offset from the dynamical center of the galaxy (Matsumoto et al. 2001).

One interpretation of these X-ray sources is that they are accretions onto intermediate-mass black holes of (10^2–10^3) $M_\odot$, while there are other possibilities, including beaming, super-Eddington accretion, and a young supernova remnant in a dense interstellar medium. Probably they do not form a single class of X-ray sources. The spectra of many of these sources can be described by a multicolor disk blackbody model with or without an additional hard tail (Makishima et al. 2000; Colbert & Mushotzky 1999). The inner disk temperatures of the sources studied by Makishima et al. (2000) are $kT \sim 1.1$–1.8 keV. Since these temperatures are higher than that from an intermediate (10^2 $M_\odot$) black hole accretion, they proposed a picture of a spinning (Kerr) black hole with a much smaller inner disk radius than that of a nonspinning (Schwarzschild) one.

The luminous X-ray source in the star-forming dwarf galaxy Holmberg II (UGC 4305) is peculiar among these cases in terms of the nature of the host galaxy and the location of the X-ray source. The galaxy is nearby at a distance of 3.05 Mpc, which was derived from Cepheid observations (Hoessel, Saha, & Danielson 1998). It is a dwarf irregular galaxy in the M81 Group with ongoing star formation activity. As in other galaxies of this class, numerous H II regions are scattered throughout the galaxy (Hodge, Strobel, & Kennicutt 1994). The bright X-ray source, which has been cataloged in the *ROSAT* bright survey (RBS; Schwope et al. 2000), is one of the most luminous X-ray sources seen in dwarf galaxies ($L_x \sim 10^{40}$ ergs s^{-1}).

It was observed three times with the *ROSAT* Position Sensitive Proportional Counter (PSPC) as pointed observations and once with HRI. Zezas, Georgantopoulos, & Ward (1999, hereafter ZGW) studied the *ROSAT* data on this X-ray source. Their main conclusions were the following: (1) The X-ray source seems pointlike and located near the edge of the galaxy. Its position is consistent with one of the compact H II region complexes of the galaxy, considering an uncertainty of $\sim 6''$ for the *ROSAT* absolute astrometry from its star tracker. A chance spatial coincidence of this H II region with an unrelated X-ray source of this brightness is highly unlikely ($\sim 3 \times 10^{-6}$). (2) The source is time variable on scales of days and years. (3) The spectrum

[1] Current address: Astrophysikalisches Institut Potsdam.

TABLE 1
LOG OF *ROSAT* AND *ASCA* OBSERVATIONS

Detector, Mode, Sequence	Start Date	Exposure (ks)
ROSAT PSPC:		
rp600140n00	1992 Apr 14	7.3
rp600431n00	1992 Oct 29	11.6
rp600431a00	14 Mar 14	3.7
ROSAT HRI:		
rh600745n00	1994 Oct 17	7.8
ASCA GIS (PH):		
ad77075000	1999 Oct 21	16.5
ASCA SIS (1-CCD/FAINT):		
ad77075000	1999 Oct 21	16.5 (S0), 16.3 (S1)

is soft and can be fitted with a steep power law ($\Gamma \sim 2.7$) or a thermal plasma (Raymond-Smith) of $kT \sim 0.8$ keV. Time variability suggests an accretion onto a compact object, but the luminosity is 2–4 orders of magnitude larger than typical X-ray binaries.

There is a radio knot that is cospatial with the H II region in the X-ray source region. It is one of the three showing radio spectra suggestive of a nonthermal emission (Tongue & Westpfahl 1995), implying a recent supernova or multiple supernovae. However, currently there is no indication of a special character in the optical–radio data in this particular H II region, which is presumably associated with the compact X-ray source, unlike other knots in the galaxy.

As a part of our study of a sample of apparent non-AGN galaxies in the RBS catalog with compact luminous X-ray sources, we have made further X-ray studies of Holmberg II. In particular, we have obtained a 20 ks *ASCA* observation of this X-ray source to search for the hard X-ray signature of AGN-like activity. In this paper, we report the results from our data analysis of our *ASCA* observation and of the *ROSAT* data from archives.

The scope of the paper is as follows: In § 2, we summarize the *ASCA-ROSAT* observations and data used in our analysis. In § 3 we report our new spectral analysis of the X-ray source by a joint *ASCA-ROSAT* PSPC analysis. In § 4, we searched for an extension by applying a wobble-correction to the *ROSAT* HRI data. Long- and short-term X-ray light curves are examined in § 5. Finally the results are discussed in § 6.

2. OBSERVATIONS

Holmberg II was observed with *ROSAT* five times. First, it was bright in the *ROSAT* All-Sky Survey (Voges et al. 1999) and cataloged in the RBS (Schwope et al. 2000). It was observed three times with *ROSAT* PSPC pointed observations in 1992–1993 for 3.7–11 ks each. Also it was observed with *ROSAT* HRI for 7.8 ks. The *ROSAT* pointed data have been retrieved from the High Energy Astrophysics Archival Research Center located at NASA Goddard Space Flight Center.

The *ASCA* observation of Holmberg II has been made with a pointing at the X-ray source in 1999 as one of the accepted targets from our proposal in the *ASCA* EAO-6 (AO-7) program (principal investigator, I. Lehmann). The brightness of the source is such that we can use the SIS FAINT mode for both the medium and high bit rates with the 1-CCD mode. Thus we chose to use the 1-CCD/FAINT modes throughout. For the subsequent analysis, we use the BRIGHT2 mode data converted from the FAINT mode. For GIS, we have used the PH mode as usual. The log of *ROSAT* and *ASCA* pointed observations is shown in Table 1.

3. X-RAY SPECTRAL ANALYSIS USING *ASCA-ROSAT* PSPC

3.1. *Extracting ASCA and ROSAT Spectra*

Extraction and preparation of spectra and response matrices have been made using tools included in FTOOLS 5.0, and subsequent spectral fittings have been made using XSPEC 11. The source spectra have been extracted from event files that have been screened using the standard screening criteria. The source-spectrum extraction radii were 6′ and 3′ for the GIS and SIS, respectively. The background spectra have been extracted from off-source areas from the same detector, excluding 7′.5 and 3′.7 from the X-ray source for the GIS and SIS data, respectively. The background subtractions have been made by scaling the background spectra by the areas of extraction, as automatically made by XSPEC. Because of the brightness of the source, the analysis is little affected by the uncertainties related to background scalings. The two GIS and two SIS spectra are co-added, respectively. The background spectra and response files have been generated for the summed GIS $2+3$ and SIS $0+1$ spectra, respectively.

The *ROSAT* PSPC spectra have been extracted using an extraction radius of 1′. Background spectra have been extracted from an annular region around the source, between 1′.25 and 3′.75. One spectrum has been made for each of the three PSPC pointed observations (Table 1). We see no evidence of a spectral change among these three data sets (see below). Thus the three spectra for these three sequences have been co-added for the joint analysis with the *ASCA* data.

The *ASCA* and *ROSAT* spectra have been rebinned such that each bin contains at least 25 counts to utilize the χ^2 statistics during the spectral analysis. The source was bright enough for this rebinning process without sacrificing the resolution.

3.2. *Spectral Analysis*

The channel energy ranges used for the analysis are 0.15–2, 0.6–10, and 1.0–7 keV for the *ROSAT* PSPC, *ASCA* GIS, and *ASCA* SIS, respectively. Because of the calibration uncertainties related to the radiation damage, we have ignored *ASCA* SIS channels below 1 keV.

First, we have verified the basic fitting results of ZGW with joint fits to the three PSPC spectra, for which all model parameters are joined except for the global normalization. As observed by ZGW, slight variations of the global normalization have been observed. This is discussed in § 5. When all parameters are separately fitted for the three data sets, the best-fit parameters are always consistent within errors with the joint ones. This warrants that we can use the summed spectra for PSPC for further analysis.

Next we have made a spectral analysis of *ASCA* only (GIS and SIS). We have tried to fit the spectra with three models: A1, a single power law; A2, a thermal plasma using the XSPEC MEKAL model; and A3, a disk blackbody

(Mitsuda et al. 1984; XSPEC model *diskbb*), where "A" stands for *ASCA*. The best-fit parameters are shown in Table 2 and the fit residuals are shown in Figure 1. The single power law of photon index $\Gamma \sim 1.9$ gave the best fit without inclusion of any absorption. The photon indices for separate fits to the spectra gave $\Gamma = 1.85 \pm 0.07$ and 1.87 ± 0.07 for GIS and SIS, respectively (N_H fixed to 0). The agreement verifies the goodness of our background subtraction. The 90% upper limit to the column density of the absorbing gas was $N_H \leq 1.3\ 10^{21}$ cm^{-2}. The thermal plasma model with $kT \sim 5$ keV also gave a good fit with $\chi^2/\nu = 0.84$. We have obtained a heavy element abundance of $Z = 0.2 \pm 0.2\ Z_\odot$, which is marginally consistent with the O/H ratio of $\sim$0.4 (relative to solar) for this galaxy (Hunter & Gallagher 1985). However, note that the metallicity of the source of X-ray emission is not necessarily equal to that of some average for the H II regions scattered throughout the galaxy and that the hard X-ray mainly measures the iron abundance, which does not necessarily match with that of oxygen.

The multicolor disk blackbody model failed to fit the *ASCA* data, as shown in Figure 1*c*. Thus the disk blackbody component does not dominate the hard X-ray emission observed by our *ASCA* observation, unlike, e.g., IC 342 source 1 and NGC 1313 source B, studied by Makishima et al. (2000). The power-law index of the *ASCA* spectrum is much harder than that of the *ROSAT* PSPC spectrum ($\Gamma \approx 2.7$; ZGW), which has response in $E \lesssim 2$ keV.

Finally, we have made a joint spectral analysis using all the *ROSAT* PSPC and *ASCA* GIS/SIS data. We have summed all three PSPC spectra for the joint spectral fits. We have joined all the model parameters except for the global normalization as before. Because the *ROSAT* spectrum, covering a lower energy range, is much softer than that of *ASCA*, we have tried models with a hard power law ($\Gamma \sim 1.9$) with some soft excess and an absorbing column. Adding a softer power-law component did not give a satisfactory fit. As for the soft component, we have tried the thermal plasma and disk blackbody models. As shown in Table 2, both "power law + thermal" (J1) and "power law + disk blackbody" (J2) models gave reasonable fits. Note that the abundance of the thermal plasma has been fixed to 0.4 (see above) for J1. When this was a free parameter, the fit could not constrain it. In both J1 and J2, the

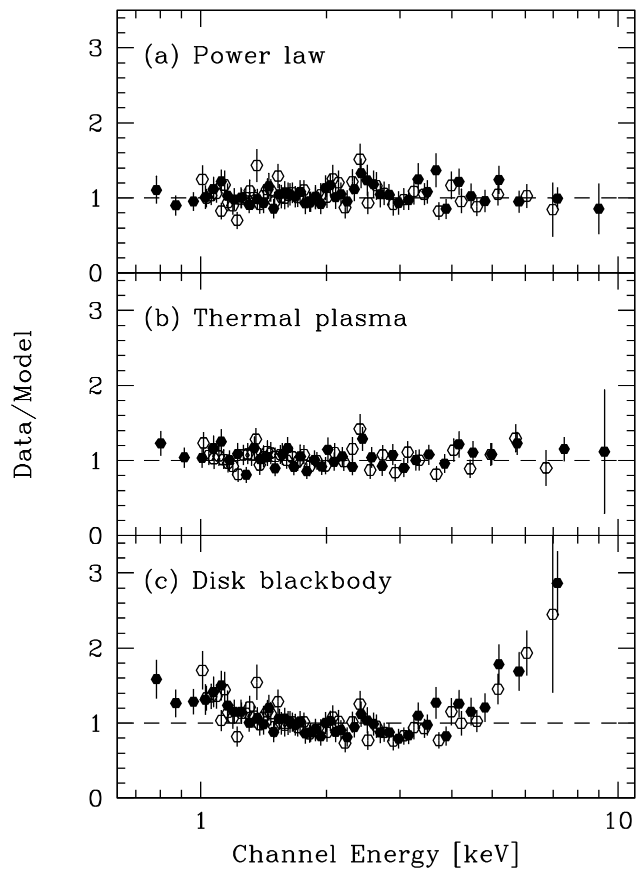

FIG. 1.—Residuals for three model fits of the *ASCA* GIS (*filled hexagons*) and SIS (*open hexagons*) spectra are shown in terms of the ratio of the data and model for (*a*) a single power-law model, (*b*) a thermal plasma model, and (*c*) a disk blackbody model. See Table 2 for the best-fit parameters.

TABLE 2

RESULTS OF THE SPECTRAL ANALYSIS

Model[a]	Parameters[b]
	ASCA GIS and SIS Data
A1 PL	$K_G = 1.0^*$; $KS = .87 \pm .05$; $\Gamma = 1.87 \pm 0.05$; $F_{p12} = 2.5 \pm 0.1$; $\chi^2/\nu = 0.83$ (170./206)
A2 Thermal	$K_G = 1.0^*$; $K_S = .86 \pm .05$; $kT = 4.8 \pm 0.4$; $F_{t12} = 2.2 \pm .1$; $Z = 0.2 \pm 0.2$; $\chi^2/\nu = 0.84$ (208./206)
A3 Disk BB	$K_G = 1.0^*$; $K_S = .87 \pm .05$; $kT_{in} = 1.19 \pm 0.05$; $F_{d12} = 1.9 \pm .1$; $\chi^2/\nu = 1.34$ (276./206)
	ROSAT PSPC and *ASCA* GIS/SIS
J1 (PL + Thermal) × Abs.	$K_G = 1.0^*$; $K_S = .87 \pm .05$; $K_P = .79 \pm .06$; $\Gamma = 1.91 \pm .04$; $F_{p12} = 2.6 \pm .2$; $kT = .30 \pm .05$; $Z = 0.4^*$; $F_{t12} = .67 \pm .17$; $N_{H_2O} = 7.9 \pm .06$; $\chi^2/\nu = 1.02$ (324./317)
J2 (PL + Disk BB) × Abs.	$K_G = 1.0^*$; $K_S = .86 \pm .04$; $K_P = .78 \pm .04$; $\Gamma = 1.88 \pm .07$; $F_{p12} = 2.6 \pm .2$; $kT_{in} = .17 \pm .02$; $F_{d12} = 1.0 \pm .2$; $N_{H_2O} = 9.6 \pm 1.1$; $\chi^2/\nu = 1.04$ (329./317)
J3 ($\mathrm{Thermal_h}$ + $\mathrm{Thermal_s}$) × Abs.	$K_G = 1.0^*$; $K_S = .87 \pm .05$; $K_P = .79 \pm .04$; $kT_h = 5.9^{+1.4}_{-.9}$; $F_{th12} = 2.0 \pm .1$; $kT_s = .35 \pm .05$; $F_{ts12} = 1.4 \pm .2$; $Z = .02^{+.03}_{-.01}$; $N_{H_2O} = 8.5 \pm 1.0$; $\chi^2/\nu = 1.00$ (317./317)

[a] (PL) Power-law model with photon index of Γ and 0.5–2 keV flux of F_{p12}; (Thermal) Thermal plasma model using the XSPEC MEKAL model with plasma temperature kT in kiloelectron volts, metal abundance Z in solar units (where the solar abundance is from Anders & Grevesse 1989), and 0.5–2 keV flux of F_{t12}—for model J3 the hard and soft thermal components are identified by subscripts *h* and *s*, respectively; (Disk BB) Multicolor disk model (XSPEC model *diskbb*; Mitsuda et al. 1984) with inner disk temperature kT_{in} and 0.5–2 keV flux of F_{m12}; (Abs) Absorption by neutral gas using the XSPEC model wabs (Morrison & McCammon 1983) with hydrogen column density $N_{H_2O}\ 10^{20}$cm^{-2}.

[b] Free parameters of fit are shown with 90% errors ($\Delta\chi^2 = 2.7$). Fixed parameter values are followed by an asterisk. K is the overall normalization factor for each detector or observation; detectors are identified by subscripts (*G* for GIS; *S* for SIS; *P* for PSPC). The normalization is expressed as a 0.5–2 keV (unabsorbed) flux in units of 10^{-12}ergs s^{-1} cm^{-2}. Reduced χ^2 values are shown in italics.

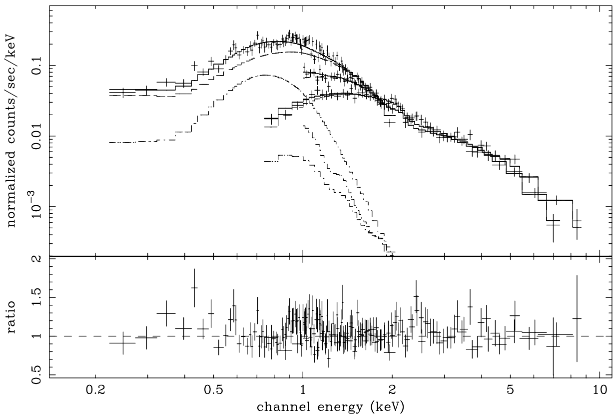

FIG. 2.—*ASCA* (GIS, 0.6–10 keV and SIS, 1–7 keV) and *ROSAT* PSPC (0.2–2 keV) spectra are shown with folded model predictions for the best-fit power-law plus thermal (MEKAL) model with absorption (fit J1). The fit residuals are shown in the lower panel in terms of the ratio of the data and the model. The error bars show 1 σ errors. The detector corresponding to each spectrum can be identified by the energy range. The power-law (*dashed line*) and thermal (*dot-dashed line*) components of the folded model have also been shown separately for each instrument.

absorbing column was $N_H \sim (0.7\text{–}1) \times 10^{21}$ cm^{-2}, which exceeds the Galactic value implied by the 21 cm data of $N_H \sim 3 \times 10^{20}$ (Dickey & Lockman 1990), indicating an absorbing component within Holmberg II. The soft excess component, which can either be described as a $kT \sim 0.3$ keV thermal plasma or a $kT_{in} \sim 0.2$ keV disk blackbody spectrum, has 20%–30% of the total 0.5–2 keV total luminosity. The *ROSAT* and *ASCA* spectra are shown with folded models and residuals in Figure 2 for J1. The total luminosity of the X-ray source is $\approx 1.0 \times 10^{40}$ ergs s^{-1} in the 0.1–10 keV range after correcting for absorption (GIS normalization). This corresponds to an Eddington luminosity of $\sim 80\ M_\odot$.

For fit J2, the GIS normalization of the disk blackbody component gives $r_{in}(\cos\theta)^{1/2} = 3500\text{–}7500$ km, where r_{in} is the inner disk radius, θ is the viewing angle, and the 90% confidence error was searched for by allowing all other variable parameters to vary. Assuming $r_{in} = 3R_S$, where R_S is the Schwarzschild radius, this corresponds to a black hole mass of (10–25)$(\cos\theta)^{-0.5}\ M_\odot$, while Colbert & Mushotzky (1999) pointed out that the r_{in} estimation based on the disk blackbody within XSPEC is likely to be underestimated. Further discussion is made in § 6

We have also tried a two–thermal plasma model fit (J3), where the relative abundances of two thermal plasmas have been fixed at equal. This model gave an acceptable fit but with a hard thermal component (thermal$_h$) with $kT_h \sim 6$ keV and a soft thermal component (thermal$_s$) with $kT_s \sim 0.3$ keV. In this case, the fitted abundance was very low, $Z = 0.02^{+.03}_{-.01}$. We did not find a satisfactory fit for the model in which the hard component is a thermal plasma and the soft component is a power law.

One caveat about our joint fitting analysis is a possible cross-calibration problem. Iwasawa, Fabian, & Nandra (1999) found that the *ROSAT* PSPC spectrum is much softer than that of *ASCA* SIS for the simultaneous observations of NGC 5548 ($\Gamma = 2.35$ for *ROSAT* PSPC versus $\Gamma = 1.95$ for *ASCA* SIS). This might have been partially caused by the soft excess combined with the spectral resolution of PSPC, or there may be real cross-calibration problems. The origin of this discrepancy is still unclear. In our case, the difference of $\Delta\Gamma \sim 0.7$ between the *ROSAT* PSPC and *ASCA* GIS spectra is much larger than that Iwasawa et al. (1999) observed for a similar *ASCA* index. Thus there certainly is a soft component in addition to the extrapolation of the hard power law even in case the discrepancy observed by Iwasawa et al. (1999) was solely caused by calibration problems.

4. *ROSAT* HRI WOBBLE-CORRECTION AND SPATIAL EXTENSION

There are wobble phase–dependent systematic errors with the aspect solution for the *ROSAT*, which could lead

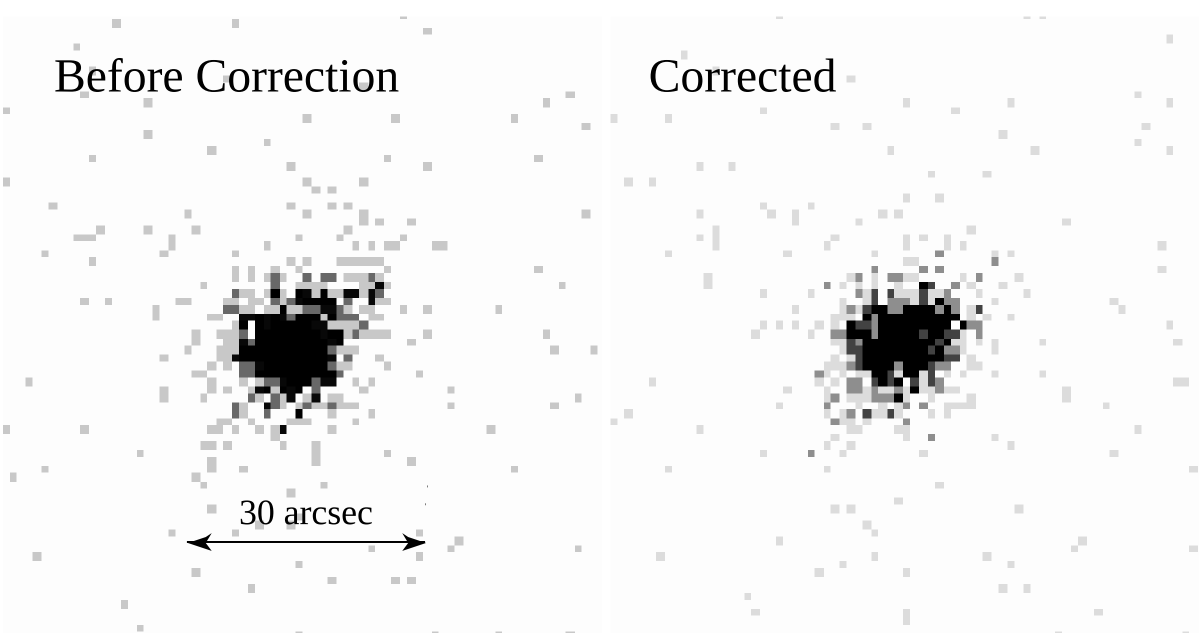

FIG. 3.—*ROSAT* HRI image of Holmberg II before and after the wobble-aspect correction. North is up, and east is left. Note that a faint knot seen at the northwest in the original image has disappeared after the correction.

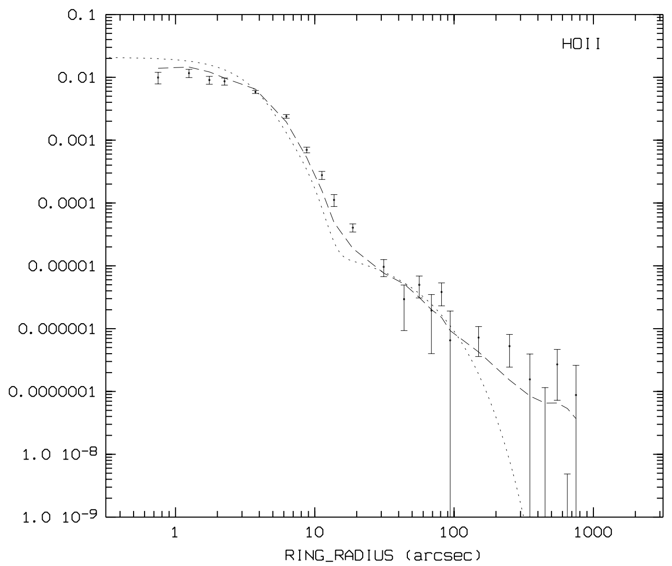

FIG. 4.—Wobble-corrected radial profile of the compact X-ray source in Holmberg II compared with the theoretical HRI PSF (*dotted line*) and the recalibrated HRI PSF (*dashed line*). The bars mark 1 σ errors of the data points. An extended component is clearly seen in $\gtrsim 10''$.

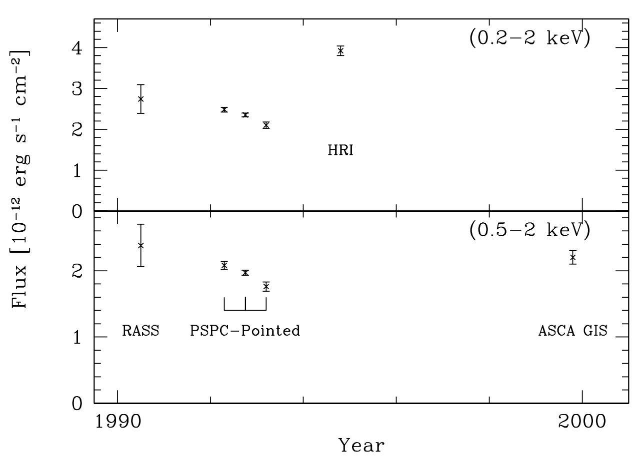

FIG. 5.—Long-term light curves of Holmberg II from 1990 to 1999 in the 0.2–2 keV (*ROSAT* PSPC and HRI) and 0.5–2 keV (*ROSAT* PSPC and *ASCA* GIS) bands. The error bars are 1 σ.

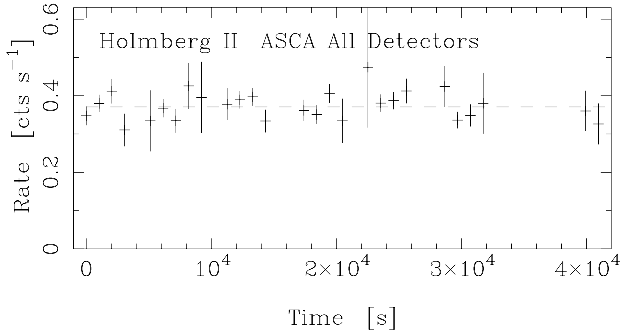

FIG. 6.—*ASCA* light curve of Holmberg II with 1 σ errors, showing the best-fit constant value (*dashed line*). Background-subtracted source counts for all four detectors have been co-added. The energy ranges are 0.6–10 and 0.7–7 keV for the GIS and SIS, respectively.

to a detection of a spurious extended component in the HRI data (Harris et al. 1998; Morse 1994). This has led ZGW to make the conservative conclusion that they had detected no extension in the HRI image. We have applied a correction for this effect by creating images in 10 wobble phases, centering each of these images independently and reconstructing the image using the centering information from Lehmann et al. (1999). The original and corrected HRI images are shown in Figure 3. The faint knot seen in the northwest in the original HRI image has disappeared in the corrected image. This reconstruction worked very well down to an HRI count rate of ~ 0.1 counts s^{-1} for a large number of stars but can be used even for fainter sources (Crawford et al. 1999).

The radial profile of the wobble-corrected HRI image has been compared with the theoretical HRI point-spread function (PSF) from David et al. (1995) and the recalibrated HRI PSF in Figure 4. The recalibrated HRI PSF was derived from wobble-corrected HRI images of 21 stars from the RBS (Schwope et al. 2000). The recalibrated HRI PSF shows a slight deviation from the theoretical PSF in the radial range between $10''$ and $30''$. The comparison of the radial profile with both PSFs indicates an extended component. After subtracting the recalibrated PSF 27% $\pm$ 5% (1 σ error) of the X-ray emission is in the extended component, and most of the excess comes from a radius of $\sim 10''$, corresponding to ~ 150 pc.

5. VARIABILITY

The *ASCA* GIS flux in the 0.5–2 keV band calculated using the spectral model J1 has been compared with the previous *ROSAT* observations. Because *ASCA* GIS is sensitive only above 0.6 keV, while *ROSAT* HRI has no spectral resolution and sensitivity in the range 0.2–2 keV, we have made separate long-term light curves for the 0.2–2 and 0.5–2 keV bands. These are shown in Figure 5. The fluxes from *ROSAT* are slightly different from Figure 3 of ZGW, probably because of the difference in spectral models. As seen in Figure 5, there is a 30% decrease in flux between the first (1992 April) and third (1993 March) PSPC pointed observations and a factor of ~ 2 increase toward the HRI observation (1994 October). The source brightness came back to a flux close to the PSPC observation during the *ASCA* observation in 1999. This does not necessarily mean that the source is variable on a timescale of years, rather it means that there is a variability at a timescale longer than the elapsed time of a single observation (10^5–10^6 s).

We also searched for evidence of time variability in the *ASCA* data. First, we have defined the combined good time intervals (GTI), which consist of the intersection of GTIs from all the SIS and GIS detectors. We have used channels corresponding to 0.6–10 keV for the GISs and to 0.7–7 keV for the SISs, respectively. For each detector, binned source and background light curves have been extracted using a 1024 s bin size. The extraction regions are the same as those of the spectral analysis. For each time bin, only the intervals overlapped with the combined GTI have been used to calculate the count rate. The background-subtracted light curves have been co-added to make the final light curve. There is no significant correlation between the background-subtracted source light curve and the background light curve. This also warrants the goodness of the background subtraction.

The resulting light curve is shown with the best χ^2 fit constant value in Figure 6. No point is more than 2 σ away from the constant value, and $\chi^2/\nu = 22.2/26$. Thus there is no evidence for variability at timescales between 10^3 and 10^4 s in the *ASCA* data. Separate light curves for the hard ($E \geq 2$ keV) and soft ($E < 2$ keV) bands did not show any sign of variability either. This is in contrast to the *ROSAT* light curves reported by ZGW, which show a convincing case of gradual decrease of flux by a factor of ~ 3 over 2×10^5 s during the second pointed PSPC observation and less convincing indications of shorter timescale variabilities.

6. DISCUSSION

Our analysis suggests at least two components of the X-ray emission. An extended and a pointlike component have been revealed by the spatial analysis. The variability also provides evidence for at least a compact component. The joint *ASCA-ROSAT* spectral analysis suggests a nonthermal power-law component plus a warm thermal component or a moderately low-temperature disk blackbody component. The overall spectrum can also be described as a superposition of two thermal components with a very low metallicity. However, the variability observed in this object argues against exclusive thermal origin of the X-ray source.

The X-ray source at the edge of Holmberg II shows unusual characteristics, even given the large number of off-nuclear X-ray sources in nearby galaxies at similar luminosities. While most of the X-ray sources studied by Colbert & Mushotzky (1999) reside in the nuclear region, this is at the very edge of a dwarf galaxy. Unlike a number of off-nuclear sources studied by Makishima et al. (2000), hard X-ray emission is not dominated by a disk blackbody component with $kT_{\rm in} \gtrsim 1$ keV. If the soft excess component comes from a disk blackbody emission, the implied black hole mass from the normalization of this component is (10–25)$(\cos\theta)^{-0.5}$ $M_\odot$, assuming a Schwarzschild black hole (see § 3). However, by estimating the mass from the temperature $kT_{\rm in} \sim 0.2$ keV by using equation (12) of Makishima et al. (2000), we obtain $\sim 10^4$ $M_\odot$. This large discrepancy argues against the disk blackbody interpretation of the soft excess, even though we consider the underestimation of the mass pointed out by Colbert & Mushotzky (1999), nearly edge-on viewing angle, and spinning of the black hole.

One of the most surprising results from our analysis is that these two (or more) bright X-ray components coexist in a compact region in one of the numerous H II regions and that no other X-ray source with a comparable brightness exists in other parts of the galaxy. All other X-ray sources scattered throughout the galaxy, which are either supernova remnants or X-ray binaries, have luminosities of $L_{\rm x} \lesssim 10^{37}$ ergs s^{-1} cm^{-2} (Kerp & Walter 2001). Thus it is unlikely that the two (or more) components have independent origins. The possible explanations of this X-ray source with observed multiple components are the following:

1. A supernova remnant (SNR) or a composite of SNRs (the $kT \sim$ 0.3 keV extended thermal component) feeds gas into an intermediate-mass black hole.
2. An accretion onto a stellar-mass compact object, e.g., similar to Galactic black hole X-ray binaries, beaming toward our line of sight, is embedded in an SNR or a composite of SNRs.
3. The nonthermal power-law and the soft excess components (possibly blackbody emission from the accretion disk around an intermediate-mass black hole) come from the same compact region, while the extended component is caused by scattering or reflection of the central source.

The flat radio spectrum (Tongue & Westpfahl 1995) in the region of this X-ray source shows the existence of a supernova remnant or a composite of supernova remnants. This supports possibilities (1) and (2). However, the extended component is too luminous for thermal emission from a single or a few SNRs, considering its size of ~ 200 pc and its 0.5–2 keV luminosity of a few times 10^{39} ergs s^{-1}. A single SNR can be at this luminosity only when it is very young ($\lesssim 10^2$ yr; Schlegel 1994; Schlegel et al. 1999), and thus it cannot have grown into this scale size nor can it feed the intermediate-mass black hole located 200 pc away. Thus more than a few supernova remnants are needed to make the extended structure, which also feeds the black hole causing the variable, nonthermal emission. From our current data, we are not able to distinguish whether the central source represents an accretion onto an intermediate-mass black hole or a stellar-mass compact object (e.g., X-ray binaries) with beaming toward our line of sight.

Possibility (3) is not likely. The possibility that electron scattering by surrounding diffuse gas is the origin of the extended emission has the following difficulty. Scattering gas with a column density of $N_{\rm H} \gtrsim 10^{23}$–$10^{24}$ cm^{-2} is required to account for the $\sim 30\%$ extended component. The gas would cause heavy photoelectric absorption unless the scattering diffuse gas is highly ionized (Wilson et al. 1992; Elvis et al. 1990). If the gas was thermally ionized, the temperature of the gas must be greater than a few million kelvins so that the absorption features due to a column density of $N_{\rm H} = 10^{23}$ cm^{-2} are not visible in the *ASCA* spectrum. For a demonstration, we assume a uniform sphere of gas 200 pc in radius filled with hot ionized gas with a column density of $N_{\rm H} = 10^{23}$ cm^{-2} from the central source. Such a sphere of thermal gas would produce X-ray emission that is several orders of magnitude larger than that observed. Photoionization also cannot be a valid explanation, because the lower limit of the ionization parameter required to be consistent with the *ASCA* spectrum also requires several orders of magnitude larger luminosity for the ionizing source. We also consider a picture in which the surfaces of optically thick molecular clouds scattered throughout the region (giant molecular clouds where star-forming activities are embedded) reflect the radiation from the central source, while our line of sight to the central source is not blocked by any of them. This picture also has a similar difficulty. To attain sufficient reflectivity in the *ROSAT* band ($E \lesssim 2$ keV), the surfaces of the clouds have to be highly ionized. Using the XSPEC model PEXRIV (Magdziarz & Zdziarski 1995), we estimate that an ionization parameter of $\xi \equiv L/(nR^2)$ of more than a few hundred ergs cm s^{-1} is required to have the reflectivity of more than 20%–30% in this band. For a central ionizing source luminosity of L about a few times 10^{40} ergs s^{-1} at a distance of $R = 200$ pc this ionization parameter corresponds to a gas density of $n \lesssim 10^{-3}$ cm^{-3} at the surfaces of the clouds. This is much lower than that of a usual interstellar medium, and scattered clouds of this density cannot be optically thick.

If the intermediate-mass black hole picture of this X-ray source is the case, there is a question of its formation. Taniguchi et al. (2000) discussed possible origins of the off-nucleus "intermediate-mass" black holes presumably responsible for off-nuclear luminous X-ray sources, and their preferred model was that of multiple mergings of stellar remnants (stellar-mass black holes and neutron stars). Matsushita et al. (2000) found a molecular superbubble in the vicinity of a similar off-nuclear X-ray source in M82, suggesting that an intensive star formation is connected to the formation of an intermediate-mass black hole. This may be the case for the compact component of the X-ray source discussed here because of the intense star-forming activity in the region. However, the question remains as to why there is only one such X-ray source in this galaxy and not at the locations of other numerous H II regions. Probably the X-ray emission is a short-lived phenomenon, in which an intermediate-mass black hole (similar things may exist in many star-forming regions) is fed by the passing of a shell of dense gas induced by multiple supernova explosions.

Chandra (scheduled as a guaranteed time target by S. Murray) and *XMM-Newton* (guaranteed time target by M. Watson) observations of this source will certainly improve our knowledge of this peculiar X-ray source. The *Chandra* observation can make spatially resolved X-ray spectroscopy and reveal whether the nonthermal component corresponds to the point source and the thermal to the extended component or if it has a more complicated structure. The *XMM-Newton* observation would give a better spectral information with much better statistics and much less cross-calibration uncertainties in the $E \lesssim 1$ keV region, where multiple components are apparent. It will also give variability information at short timescales.

7. CONCLUSIONS

We summarize the main conclusions of our analysis:

1. New *ASCA* and archival *ROSAT* data of the X-ray source in Holmberg II have been analyzed.
2. The combined *ASCA* and *ROSAT* spectrum shows the X-ray source can be described as a $\Gamma \sim 2$ power law and a soft excess that can be described either as a $kT \sim 0.3$ keV thermal plasma or a $kT_{\rm in} \sim 0.2$ disk blackbody. We argue against the disk blackbody interpretation of the soft excess component based on the inconsistency between the luminosity and the temperature.
3. The wobble-corrected *ROSAT* HRI image indicates $\sim$25% of the X-ray emission is extended on a scale of $\gtrsim 10''$ ($\sim$25%). Variability in the *ROSAT* data shows that the pointlike component probably comes from accretion onto a compact object.
4. It is remarkable that this multiple-component X-ray source is the only one of such strength among the numerous H II regions in the galaxy with a similar nature. It is natural to suppose that these two components are related.
5. Possible explanations of the nature of the X-ray source include multiple supernova remnants (extended component) feeding the accretion onto an intermediate-mass black hole. We cannot, however, exclude the possibility that the central source is caused by beamed radiation from an accretion onto a stellar-mass (usual X-ray binaries) object. We argue against a picture in which electron scattering or reflection by scattered optically thick clouds of the central source makes the extended X-ray emission.

This research has made use of data and software obtained from the High Energy Astrophysics Archival Research Center located at NASA Goddard Space Flight Center. The authors appreciate the effort of *ASCA* and *ROSAT* teams in having created and operated these superb observatories. The authors thank the referee, Hironori Matsumoto, for his careful review and useful comments.

REFERENCES

Anders, E., & Grevesse, N. 1989, Geochim. Cosmochim. Acta, 53, 197
Colbert, E. J. M., & Mushotzky, R. F. 1999, ApJ, 519, 89
Crawford, C. S., Lehmann, I., Fabian, A. C., Bremer, M. N., & Hasinger, G. 1999, MNRAS, 308, 1159
David, L. P., Harnden, F. R., Kearns, K. E., & Zombek, M. V. 1995, The *ROSAT* High Resolution Imager (Cambridge, MA.: Smithsonian Astrophysical Observatory)
Dickey, J. M., & Lockman, F. J. 1990, ARA&A, 28, 215
Elvis, M., Fassnacht, C., Wilson, A. S., & Briel, U. 1990, ApJ, 361, 459
Fabbiano, G. 1989, ARA&A, 27, 87
Harris, D. E., Silverman, J. D., Hasinger, G., & Lehmann, I. 1998, A&AS, 133, 431
Hodge, P., Strobel, N. V., & Kennicutt, R. C. 1994, PASP, 106, 309
Hoessel, J. G., Saha, A., & Danielson, G. E. 1998, AJ, 115, 573
Hunter, D. A., & Gallagher, J. S. 1985, ApJS, 58, 533
Iwasawa, K., Fabian, A. C., & Nandra, K. 1999, MNRAS, 307, 611
Kerp, J., & Walter, F. 2001, in ASP Conf. Ser. 234, X-Ray Astronomy 2000, ed. R. Giacconi, L. Stella, & S. Serio (San Francisco: ASP), in press
Lehmann, I., Hasinger, G., Schwope, A. D., & Boller, T. 1999, in Highlights in X-Ray Astronomy, ed. B. Aschenbach & M. Freyberg (MPE Rep. 272) (Garching: MPE Extraterr. Phys.), 209
Magdziarz, P., & Zdziarski, A. A. 1995, MNRAS, 273, 837
Makishima, K., et al. 2000, ApJ, 535, 632
Matsumoto, H., & Tsuru, T. G. 1999, PASJ, 51, 321
Matsumoto, H., Tsuru, T. G., Koyama, K., Awaki, H., Canizares, C. R., Kawai, N., Matsushita, S., & Kawabe, R. 2001, ApJ, 547, L25
Matsushita, S., Kawabe, R., Matsumoto, H., Tsuru, T. G., Kohno, K., Morita, K., Okumura, S. K., & Vila-Vilaró, B. 2000, ApJ, 545, L107
Mitsuda, K., et al. 1984, PASJ, 36, 741
Morrison, R., & McCammon, D. 1983, ApJ, 270, 119
Morse, J. A. 1994, PASP, 106, 675
Ptak, A., & Griffiths, R. E. 1999, ApJ, 517, L85
Read, A. M., Ponman, T. J., & Strickland, D. K. 1997, MNRAS, 286, 626
Schlegel, E. M. 1994, ApJ, 424, L99
Schlegel, E. M., Ryder, S., Staveley-Smith, L., Petre, R., Colbert, E., Dopita, M., & Campbell-Wilson, D. 1999, AJ, 118, 2689
Schwope, A. D., et al. 2000, Astron. Nachr., 321, 1
Taniguchi, Y., Shioya, Y., Tsuru, T. G., & Ikeuchi, S. 2000, PASJ, 52, 533
Tongue, T. D., & Westpfahl, D. J. 1995, AJ, 109, 2462
Voges, W., et al. 1999, A&A, 349, 389
Wilson, A. S., Elvis, M., Lawrence, A., & Bland-Hawthorn, J. 1992, ApJ, 391, L75
Zezas, A. L., Georgantopoulos, I., & Ward, M. J. 1999, MNRAS, 308, 302 (ZGW)